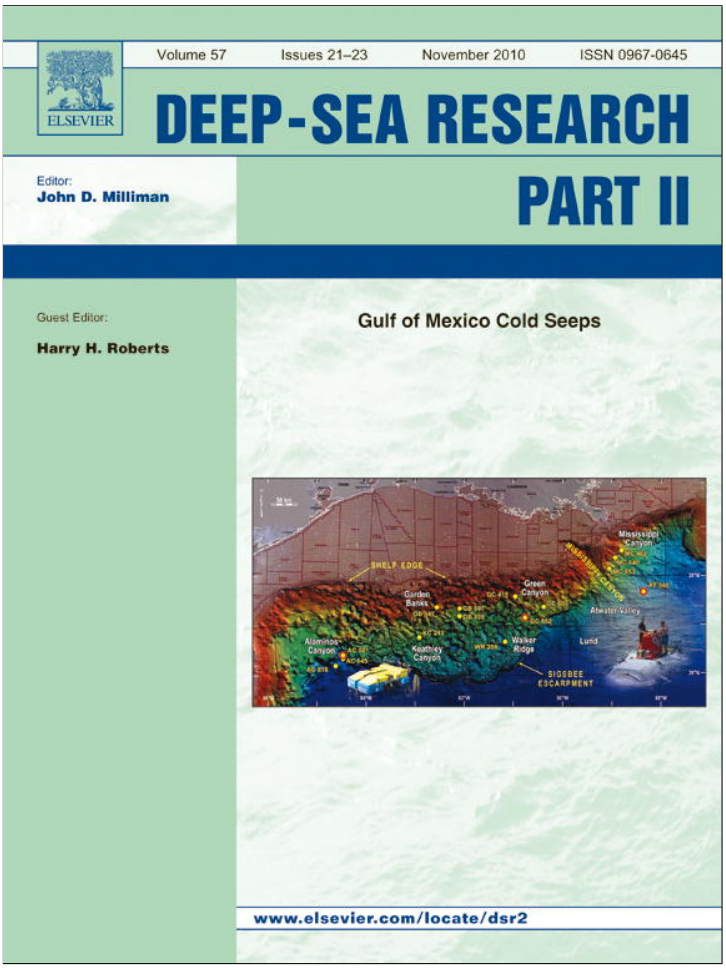

Deep-Sea Research II 57 (2010) 2022–2029

Contents lists available at ScienceDirect

Deep-Sea Research II

journal homepage: www.elsevier.com/locate/dsr2

New constraints on methane fluxes and rates of anaerobic methane oxidation in a Gulf of Mexico brine pool via *in situ* mass spectrometry

Scott D. Wankel [a], Samantha B. Joye [b], Vladimir A. Samarkin [b], Sunita R. Shah [c], Gernot Friederich [d], John Melas-Kyriazi [e], Peter R. Girguis [a,*]

[a] Department of Organismic and Evolutionary Biology, Harvard University, Cambridge, MA 02138, USA
[b] Department of Marine Sciences, University of Georgia, Athens, GA 30602-3636, USA
[c] US Naval Research Laboratory, Washington DC 20375, USA
[d] Monterey Bay Aquarium Research Institute, Moss Landing, CA, USA
[e] Stanford University, Stanford, CA 94305, USA

ARTICLE INFO

Article history:
Received 10 May 2010
Accepted 10 May 2010
Available online 14 August 2010

Keywords:
Methane flux
Mass spectrometer
Brine pool
Methane oxidation
Gulf of Mexico

ABSTRACT

Deep-sea biogeochemical cycles are, in general, poorly understood owing to the difficulties of making measurements *in situ*, recovering samples with minimal perturbation, and, in many cases, coping with high spatial and temporal heterogeneity. In particular, biogeochemical fluxes of volatiles such as methane remain largely unconstrained because of the difficulties with accurate quantification *in situ* and the patchiness of point sources such as seeps and brine pools. To better constrain biogeochemical fluxes and cycling, we have developed a deep-sea in situ mass spectrometer (ISMS) to enable high-resolution quantification of volatiles in situ. Here we report direct measurements of methane concentrations made in a Gulf of Mexico brine pool located at a depth of over 2300 m. Concentrations of up to 33 mM methane were observed within the brine pool, whereas concentrations in the water directly above were three orders of magnitude lower. These direct measurements enabled us to make the first accurate estimates of the diffusive flux from a brine pool, calculated to be 1.1 ± 0.2 mol m^{-2} yr^{-1}. Integrated rate measurements of aerobic methane oxidation in the water column overlying the brine pool were $\sim$320 μmol m^{-2} yr^{-1}, accounting at most for just 0.03% of the diffusive methane flux from the brine pool. Calculated rates of anaerobic methane oxidation were 600–1200 μM yr^{-1}, one to two orders of magnitude higher than previously published values of AOM in anoxic fluids. These findings suggest that brine pools are enormous point sources of methane in the deep sea, and may, in aggregate, have a pronounced impact on the global marine methane cycle.

1. Introduction

1.1. Global importance of methane

The marine methane cycle has been the subject of much investigation in recent years, in large part because of burgeoning interest and concern over deep-ocean methane hydrates. The deep-ocean methane reservoir represents an enormous and dynamic pool of carbon, likely exceeding reserves of conventional oil and gas (Collett and Kuuskraa, 1998). In deep-ocean regions, characterized by low temperatures, high pressure, and sufficient methane concentration, methane exists largely in the solid form of a gas hydrate (Kvenvolden, 1993). Methane seeps and associated gas hydrates have been identified along many passive and active continental margins (Kvenvolden and Lorensen, 2008). Because the destabilization of hydrates is sensitive to increases in temperature or decreases in pressure, it has been postulated that increases in mean global temperatures might trigger a release of methane into the ocean and atmosphere. A significant release of methane into the atmosphere could ultimately lead to a catastrophic greenhouse effect; this mechanism has been invoked as an explanation for past deglaciation events (Dickens, 2003; Sloan et al., 1992; Zachos et al., 2001).

Despite numerous recent studies of methane hydrates, modern fluxes of methane from the deep sea into surface waters and ultimately the atmosphere are very poorly constrained. Estimates of methane flux have been aided, to some degree, by recent advances in our understanding of marine microbiological influences on the global methane cycle. Aspects of the marine methane cycle remain largely unconstrained owing to limitations in methods and technologies that enable accurate assessment of methane concentration and flux, as well as rates of biological

* Corresponding author. Tel./fax: +1 781 874 9137.
E-mail address: pgirguis@oeb.harvard.edu (P.R. Girguis).

0967-0645/$ - see front matter © 2010 Elsevier Ltd. All rights reserved.
doi:10.1016/j.dsr2.2010.05.009

methanogenesis or methanotrophy. Pressure and temperature have a pronounced effect on methane solubility. Therefore, upon retrieval of methane-saturated waters or hydrate-rich sediments from the deep ocean, methane rapidly outgasses to the atmosphere. Thus it has been challenging to constrain flux and microbial activity *in situ*, under environmentally relevant conditions. Because previous data have shown that methane oxidation, both aerobic and anaerobic, are the largest methane sinks in marine environments (Reeburgh, 2007), understanding what controls methane oxidation, including concentration and abiotic flux, is paramount to understanding global methane dynamics.

To better constrain the methane flux in chemically reducing environments, and ultimately to quantify the influence of biotic and abiotic processes on the methane cycle, we employed a newly developed *in situ* mass spectrometer (ISMS) to conduct direct measurements of methane concentration which, in concert with shipboard microbiological measurements, were used to generate more robust estimates of diffusive flux and net methane oxidation rates in a newly discovered brine pool in the Gulf of Mexico.

2. Geologic setting

Along the continental shelf in the Gulf of Mexico, massive reservoirs of liquid and gaseous hydrocarbons lie buried beneath kilometers of sediment accumulated from the Mississippi River drainage basin. Owing to compression and dewatering of the overlying sediments, underlying evaporite deposits have undergone plastic deformation, resulting in salt-diapir driven tectonic activity (Kennicutt et al., 1988). The resulting system of fractures and faults provides conduits for the emission of hydrocarbons to the seafloor via seepage (Roberts and Carney, 1997). Hydrocarbon seeps are often characterized by abundant chemosynthetic-based macro- and microfaunal communities, including tubeworms, mussel beds, and bacterial mats, which thrive on the reduced organic compounds emanating from below (Fisher et al., 2007; MacDonald et al., 1990; MacDonald et al., 2003). In addition, hypersaline brine fluids seep from the seafloor in many locations (MacDonald et al., 1990; Joye et al., 2005, 2009). Previous studies have provided insight into the geochemical composition of these brine pools, though to date volatile flux and net rates of methane oxidation remain poorly constrained. Because of the challenges in quantification resulting from off-gassing ((at *in situ* pressures and temperatures relevant here, methane saturation is $\sim$174 mmol kg^{-1} (Duan and Mao, 2006)). Accurate sampling of fluids with high gas content using conventional methods (e.g., Niskin Bottles) has thus proven impractical for volatiles.

The brine pool characterized in this study (AC601) is located in Alaminos Canyon lease block 601 (26° 23.53N 94° 30.85W) (Roberts et al., 2007; Roberts and Boland, 2010). The brine pool is estimated to be $\sim$250 m in diameter and approximately 2334 m below the sea surface. This brine pool was visited during expeditions on board the *RV Ronald H. Brown* using the *DSV Jason II* during expeditions from May 6 through June 4, 2006, and June 3 through July 6, 2007 (see Roberts and Boland, 2010), for further description of the expeditions and site locations). Discrete geochemical measurements of this brine pool were made during the 2006 and 2007 expeditions, and deployment of the ISMS was carried out during the 2007 expedition.

3. Methods

3.1. Fundamentals of Membrane Inlet Mass Spectrometry/ISMS

Over the past five decades, the use of Membrane Inlet Mass Spectrometry (MIMS) has proven to be a powerful tool for measuring complex mixtures of dissolved gases in both industrial and laboratory settings (Johnson et al., 2000; Ketola et al., 2002). MIMS represents an optimal technique for mixed-environment gas analysis, having a high degree of sensitivity and precision, with minimal sample perturbation (Kana et al., 1994). It has been used over the past several decades to measure and monitor a wide range of dissolved gases in aquatic and terrestrial environments, including bacterial mats, peat bogs, estuarine sediments, forest soils, and tree canopies, to name a few (Hemond, 1991; Kana et al., 1998; Lloyd et al., 1986, 1998). MIMS has also been used to study metabolite flux during shipboard high-pressure experiments (e.g., Girguis et al., 2000, 2002). It has emerged as an important tool for analyzing dissolved gases in seawater (e.g., dissolved gases in surface waters analyzed continuously aboard ship (Kaiser et al., 2005; Tortell, 2005a,b) and more recently for *in situ* marine surface waters (Bell et al., 2007; Camilli and Hemond, 2004; Kaiser et al., 2005; Tortell, 2005a, b).

The recent adaptation of MIMS to *in situ* environmental analyses demonstrates the utility of such an instrument operating while underway at se, allowing the continual monitoring of many gas species in real time. This approach allows highly accurate monitoring of spatially explicit biogeochemical changes. For example, changes in O_2/Ar indicate alterations in net community production in ocean surface waters in different regions of the eastern equatorial Pacific (Kaiser et al., 2005). Additionally, N_2/Ar has been used to identify areas of active denitrification (e.g., N_2 production) in seasonally oxygen-depleted bottom waters via MIMS in Saanich Inlet (Tortell, 2005b). Underway shipboard trace gas analysis has also shed light on dynamics of dimethylsulfide (Tortell, 2005a).

Given the apparent utility of real-time quantification by MIMS, we aimed to develop a MIMS that would achieve comparable performance in waters deeper than 1000 m. Currently, investigation of deepwater samples still generally requires collection of individual samples and shipboard analysis (e.g., Tortell, 2005b), risking contamination and/or degassing. Furthermore, individual sample collection and analysis can often result in delays between sampling and data interpretation. Our understanding of deep-sea biogeochemistry would greatly benefit from real-time *in situ* dissolved gas analysis. Here we present results from a real-time *in situ* membrane inlet mass spectrometer designed to (A) operate at depths of up to 450 atmospheres of pressure, (B) provide real-time data to the user (when used on human-occupied submersibles or remotely operated vehicles), and (C) enable sampling with high spatial and temporal resolution using an *in situ* pumping system.

3.2. ISMS design and calibration

This ISMS consisted of three primary subsystems: (1) a high-pressure membrane inlet (Fig. 1a) with a small-volume seawater pumping system; (2) a quadrupole mass spectrometer (Fig. 1e,f) and oil-less vacuum pumping system (Fig. 1d,g); and (3) an underwater housing (either a 2000-m-rated aluminum 3300 alloy housing or a 4500-m-rated 6AL-4 V titanium housing, both of which are approximately 120 cm in length and 24 cm in diameter). The membrane inlet assembly consisted of a circular sheet (0.625 in. diameter) of polydimethylsiloxane (PDMS) membrane structurally backed by an integrated woven fiber (Franatech, Germany). This pliable membrane material was supported by a sintered stainless steel frit (5μm pore size, Applied Porous Materials, Tariffville, CT, USA), which was in turn supported by the titanium body of the inlet housing. Sample water was pumped through the inlet housing assembly (2 ml internal volume) at a flow rate of $\sim$3 ml/min using a small

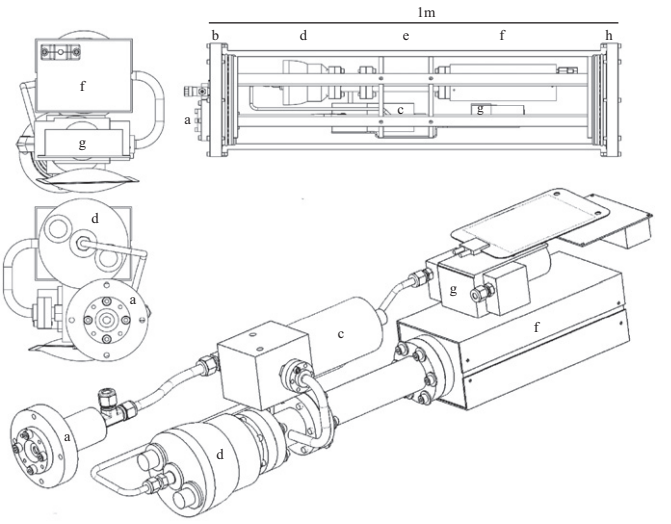

Fig. 1. Schematic of the in situ mass spectrometer. (a) membrane inlet housing, (b) front end plate of titanium pressure housing, (c) high-pressure solenoid for isolation of vacuum chamber, (d) Alcatel ATH-31+ Turbo Pump, (e) vacuum flight tube housing the SRS Quadrupole RGA-200, including ion source, quadrupoles, and detectors, (f) electronics head for controlling and reading spectrometer signals, (g) KNF Neuberger roughing pump model ANDC-84.3. Sample gas is continuously extracted across the membrane located in (a) into the high vacuum system (d, g), ionized in (e) and analyzed by the detector and electronics control unit housed in (f). The instrument is approximately 1 m in length.

solenoid pump (The Lee Company, Westbrook, CT, USA), which was controlled by an adjustable timing circuit located inside of the pressure housing.

The membrane assembly was connected to a Stanford Research Systems Residual Gas Analyzer (SRS RGA100) via standard vacuum flanges. Within the vacuum system, a pressure of $\sim$ $10e^{-5}$ Torr was maintained by a turbo-molecular pump (model: ATH 31+; Alcatel, France) backed by a diaphragm roughing pump (model: ANDC83.4; KNF- Neuberger, Trenton, NJ, USA). Open-source electron impact ionization was carried out with a thoriated iridium wire filament. The mass spectrometer and pumps were protected from membrane failure by a high-pressure/high-vacuum solenoid valve (Circle Seal, Inc., Corona, CA, USA), which is actuated upon intrusion of water. The entire mass spectrometer assembly was placed in one of the aforementioned housings. We used 24 VDC power and two independent RS-232 channels (for serial communications with the turbo pump control board and continuous feedback from the RGA analyzer), which were supplied via a wet-connect underwater cable (SubConn, Inc., North Pembroke, MA, USA). In this configuration, real-time monitoring of fluid chemistry is achievable during submersible or ROV operations, which facilitates informed site selection for fluid measurements as well as adaptive sampling of biological specimens.

To conduct the benchtop high-pressure calibrations (Fig. 2), we utilized model 110 A HPLC pumps (Beckman-Coulter, Fullerton, CA, USA) that were used to deliver calibrated solutions past the membrane surface at various flow rates and pressures. Hydrostatic pressure against the membrane inlet was manually controlled with a backpressure valve (StraVal Valve, Garfield, NJ, USA) and monitored with high-pressure gauges. Various calibration solutions were used, including air-sparged DI water or seawater, degassed distilled water and/or seawater equilibrated with gas mixtures of interest (e.g., CH_4), including use of a high pressure equilibration system for generating very high CH_4 concentrations (Fig. 2). A gas chromatograph (HP 5890 Series II plus with a TCD) outfitted with a custom gas extractor (Childress

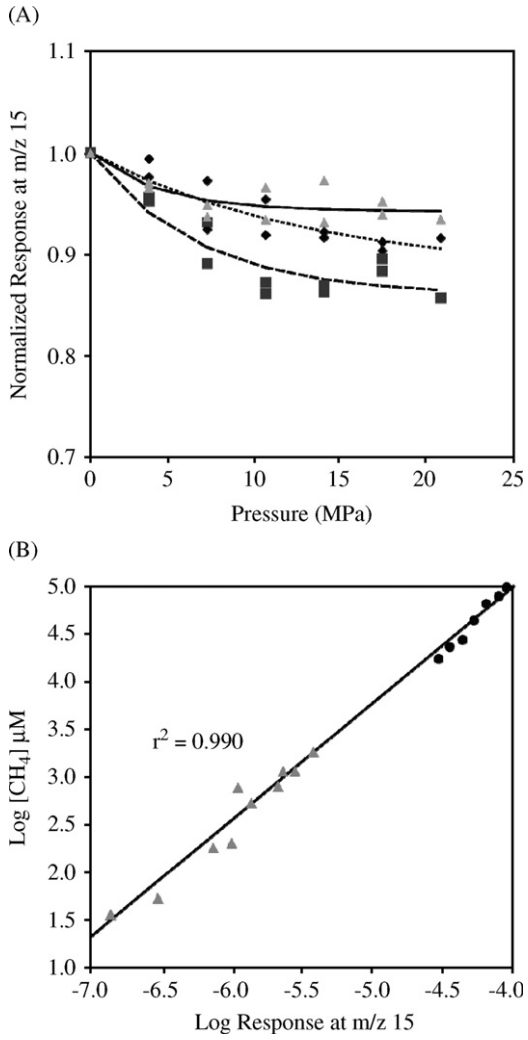

Fig. 2. (A) Normalized response at m/z 15 over a range of hydrostatic pressure for three examples fluid temperatures and concentrations, 10 °C 1160 µM CH_4 (gray squares), 2 °C 800 µM CH_4 (black triangles), and 14 °C 180 µM CH_4 (gray triangles). Responses to pressure were experimentally fit under a wide range of temperatures and concentrations (as in Bell et al., 2007) with values of b' ranging between 0.02 and 0.24 and values of k ranging between 0.84 and 0.94. (B) The response of m/z 15 (corrected for pressure effects, see (A)) was linearly proportional to methane concentrations as measured independently by gas chromatography (gray triangles) and as calculated after Duan et al., 2006, during high-pressure calibration measurements (black circles).

et al., 1984) designed for quantification of rapidly degassed seawater samples was used to obtain independent analyses of dissolved methane concentrations, and previously described equations of state were used to calculate dissolved methane concentrations at very high pressures (Duan and Mao, 2006) (Fig. 2B). During lab experiments, relative changes in signal intensity were proportional to changes in the permeation of gas through the membrane (caused by either to changes in permeate concentration or changes in the permeability coefficient). We and others have observed that changes in hydrostatic pressure can have an influence on permeation of gases through membrane materials, in particular PDMS, interpreted to be caused by compression of the membrane pore space through which analyte gas passes (Bell et al., 2007). A change in the relationship between dissolved gas concentration and signal intensity was observed during large changes in hydrostatic pressure (Fig. 2A). To account for this response, we conducted calibrations using methane dissolved in seawater over a range of *in situ* pressures and used

these results to develop an empirical correction as previously described (Bell et al., 2007). While this approach corrects for implicit changes in membrane behavior, it should be noted that the ISMS dataset presented here is comprised entirely of fluids sampled at a relatively constant depth (~2330 ± 2 m; 233 bar) and temperature; therefore, effects caused by differential pressure or temperature among the samples collected were negligible. Bench-top calibrations indicate that the accuracy of ISMS methane concentrations in the configuration described here was × 11%, primarily owing to the correction required for the pressure effects on the PDMS membrane (accuracy is improved through the use of alternate membrane material, e.g., Teflon AF). Notably, however, the precision of the ISMS measurements is much better than this finding and, based on bench-top calibrations, is within × 1%.

3.3. Water column methane and oxygen concentration

To determine brine pool and seawater column methane concentrations, a CTD rosette was lowered into the brine pool, and sonar was used to identify the brine pool as the rosette approached the bottom. Niskin bottles were tripped during descent to prevent contamination of bottles as gas came out of solution during the rosette's ascent. Two bottles were tripped in the brine pool itself, and two were tripped 1 m above the brine-seawater interface (the interface was confirmed by the real-time conductivity signal). After securing the rosette on deck, water samples were immediately transferred to 1-L PET-G bottles using gas-impermeable tubing. Bottles that were tripped in the brine were substantially over-pressured and not suitable for gas quantification (though samples were transferred to the PET-G bottles for rate measurements). A second sample was transferred to a 250-mL BOD bottle for determination of dissolved oxygen using a high-sensitivity Orion® oxygen electrode. Methane was extracted using an adaptation of the sonication/vacuum extraction technique (Suess et al., 1999) followed by gas chromatography for quantification. Prior to dissolved gas extraction, samples were stored at bottom water temperature (4 °C). Two individual samples were analyzed from each rosette bottle.

3.4. ISMS deployments and determining brine pool methane concentrations

Upon reaching the brine pool, the submersible was not allowed to disturb the brine-seawater interface. Using the ROV manipulator, the ISMS sample inlet was positioned and held in place until the ISMS response reached steady state, from which *in situ* concentrations of CH_4 were calculated. Five independent sets of measurements were made, beginning with two just above the brine fluid and three at approximate depths of 5, 20, and 80 cm into the fluid (Figs. 3 and 4).

3.5. Methane oxidation rates

Aerobic methane oxidation occurs according to the following stoichiometry:

$$CH_4 + 2O_2 \rightarrow HCO_3^- + H^+ + H_2O \quad (1)$$

Accordingly, aerobic methane oxidation rates were determined by incubating samples with C^3H_4 and tracking the production of ^3H_2O (Carini et al., 2005; Valentine et al., 2001). Typically, triplicate live and dead (Hg killed; i.e., samples were amended with $HgCl_2$ to arrest all biological activity) samples from each depth were incubated for 36 hours at *in situ* temperatures.

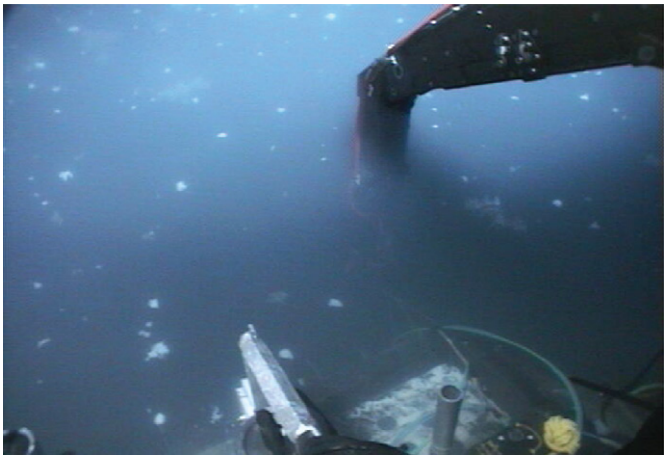

Fig. 3. Photo from the pilot cam of ROV JASON showing the starboard manipulator reaching through the seawater/brine pool interface and sampling at a depth of approximately 80 cm.

Un-reacted C^3H_4 tracer was removed by purging samples with water-saturated CH_4, and the oxidation product, ^3H_2O, was quantified by liquid scintillation counting (Carini et al., 2005).

In general, marine anaerobic methane oxidation in hydrocarbon seeps and brine pools is coupled to sulfate reduction, with the net reaction:

$$CH_4 + SO_4^{2-} \rightarrow HCO_3^- + HS^- + H_2O \quad (2)$$

Anaerobic methane oxidation rates were also determined by incubating samples with $^{14}CH_4$ and tracking the production of $^{14}CO_2$ (as in Joye et al., 1999; Valentine et al., 2001). Triplicate live and dead (Hg killed) samples from the surface (~20 cm) and subsurface (~100 cm) brine were incubated for 48 hours at *in situ* temperatures. Unreacted $^{14}CH_4$ tracer was removed by purging with water-saturated CH_4 and the $^{14}CO_2$ oxidation product was quantified following acid extraction and trapping on a phethylamine wick, followed by liquid scintillation counting (Carini et al., 2005).

3.6. Sulfate reduction rates

Samples for sulfate reduction were collected into gas-tight glass tubes, amended with radiotracer ($^{35}SO_4^{2-}$), and incubated for 24 hours (as in Joye et al., 2004; Orcutt et al., 2005). For each depth, triplicate samples were incubated alongside controls (killed at time zero). After incubation, samples were transferred from the tubes to 50-ml centrifuge tubes and mixed with 20% zinc acetate. Samples were processed and rates calculated as presented in Orcutt et al. (2005).

3.7. Major ion chemistry

Concentrations of major ions (SO_4^{2-}, Cl^-), dissolved inorganic carbon (DIC), dissolved organic matter (DOM) and dissolved inorganic nitrogen (DON) (NH_4^+, NO_2^- and NO_3^-) were determined using previously reported methods (Joye et al., 2004, 2010 and references therein).

4. Results

4.1. General geochemical composition of brine pool AC601

Geochemical data on the waters collected from the brine pool are given in Table 1. The waters of the brine pool were anoxic

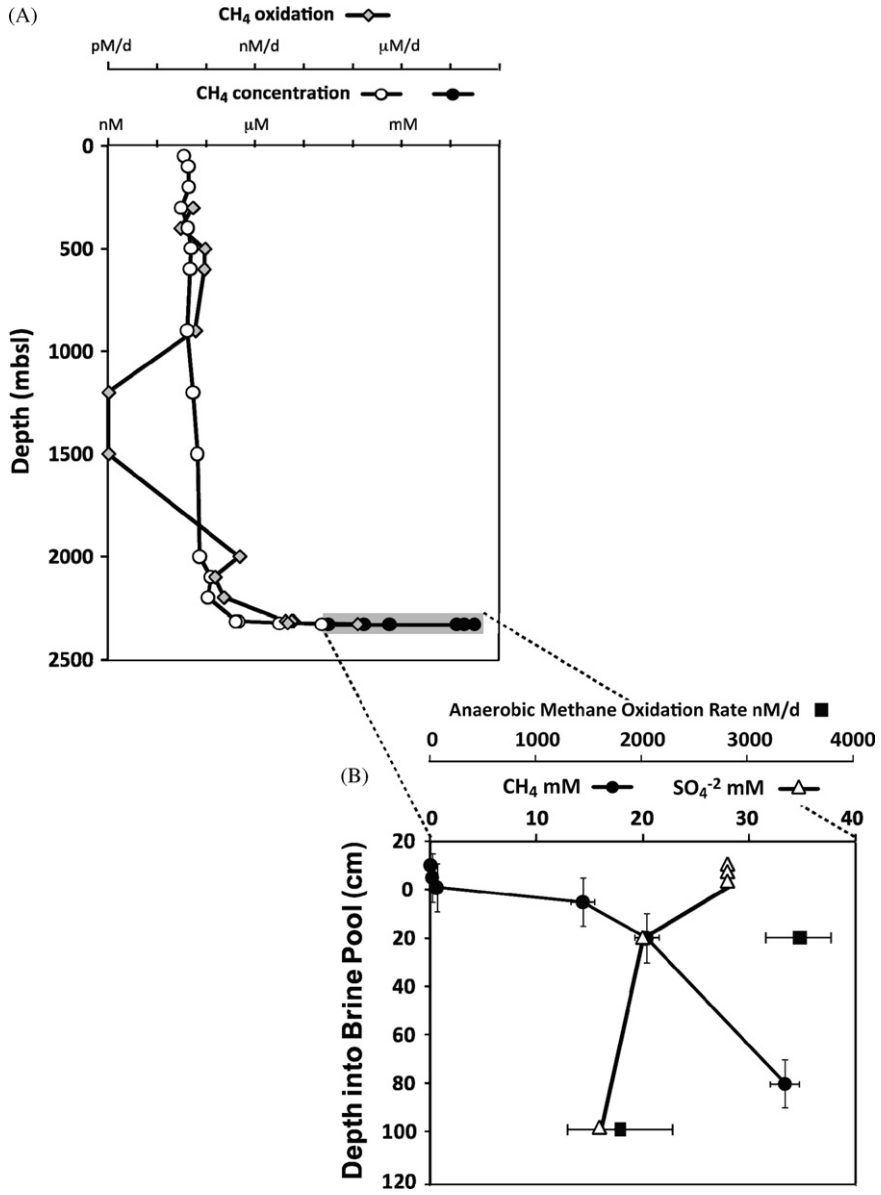

Fig. 4. (A) Depth profile of methane concentration and methane oxidation rates in the water column above brine pool AC601. Note log scale. Open circles are concentration measurements made from Niskin bottle samples; black circles are those made *in situ* using the ISMS. (B) Close up of seawater/brine pool interface and profile into the brine fluid. Note the linear scale in contrast to panel a. Measured rates of anaerobic methane oxidation (AOM) at two depths within the brine pool are shown. Note that these rates, when corrected for in situ CH_4 concentrations, are 30–45 times higher. Sulfate concentrations are depleted in the brine, consistent with their role in AOM.

($O_2 < 2\,\mu M$), with a pH of ~6.3. Salinities were substantially elevated above seawater at 82 and 92 for the 20- and 100-cm depths, respectively, with chloride measuring 1366 and 1533 mM at each depth. Water from both depths was highly enriched in dissolved inorganic carbon (DIC; 11.2 mM at 20 cm, 12.8 mM at 100 cm). Sulfate concentrations were lower than seawater, decreasing with depth into the pool (Fig. 4). Dissolved inorganic nitrogen was dominated by very high NH_4^+ (1750 and 2195 μM, 20 and 100 cm, respectively), with NO_3^- disappearing sharply in the top meter of the brine. The dissolved organic matter content was also high, with a low C:N of ~4.6, suggesting the importance of autochthonous production within the brine waters.

4.2. Water-column and brine pool CH_4 oxidation and SO_4^{-2} reduction rates

Aerobic methane oxidation rates measured in the water column above the brine pool from depths of 300 to 2313 m (or heights above the brine pool from 0 to 2013 m) ranged from 0.00 to 6.33 ± 0.9 pmol $L^{-1}\,d^{-1}$ (hereafter pM d^{-1}) (Fig. 4). The aerobic methane oxidation rate in the sample taken from directly above (~3 m) the brine pool (2328 m) was significantly higher, 129.6 ± 18.2 pM d^{-1}, than rates at any other depth. Using the methane concentrations determined via gas chromatography and the empirically derived oxidation rates, we calculate an integrated aerobic methane oxidation rate in the water column above the brine pool of 320 μmol $m^{-2}\,yr^{-1}$

Within the brine pool, two samples (20 and 100 cm) were retrieved and used for sulfate reduction and anaerobic oxidation of methane (AOM) rate measurements (Table 2). Methane concentrations measured in the bottles used for the rate measurements were 454 and 1320 μM, respectively (Table 1), giving rates at these depths of 78.8 ± 7.6 and 62.1 ± 13.1 nmol $L^{-1}\,d^{-1}$, respectively. Sulfate concentrations in the brine were depleted relative to seawater, with concentrations of 20 and 16 mM at 20 and 100 cm, respectively. Sulfate reduction rates were 107 and

Table 1
Major chemical components of brine pool AC601.

Depth cm	pH	salinity	oxygen	Concentration μM						Concentration μM						DOC:DON
				DIC	H_2S	SO_4^{2}	Cl^-	CH_4[a]	CH_4[b]	NH_4^+	NO_x	DIN	TDN	DON	DOC	
5									14.35							
20	6.29	82	<2 μM	11.2	0.00	20	1366	0.454	20.29	1750	3.4	1753.4	1843.5	90.1	423.5	4.7
80									33.29							
100	6.25	92	<2 μM	12.8	0.25	16	1533	1.320	38.40[c]	2195	0.3	2195.3	2280.5	85.2	380.0	4.5

[a] Concentrations measured via gas chromatography on samples retrieved with a CTD rosette and Niskin bottles
[b] Concentrations measured via *in situ* mass spectrometer
[c] estimated by regression of the three ISMS data points collected above.

Table 2
Rates of sulfate reduction and anaerobic methane oxidation in Gulf of Mexico brine pool AC601.

Depth cm	Rate nM/d		
	Sulfate Reduction	Anaerobic Methane Oxidation[a]	Anaerobic Methane Oxidation[b]
20	107.1 ± 14.6	78.8 ± 7.6	3502.0 ± 340
100	49.8 ± 8.4	62.1 ± 13.1	1807.4 ± 330

[a] measured using water samples collected via CTD rosette and Niskin bottles.
[b] estimated rates corrected for measured concentrations *in situ* and using rate constants measured from shipboard incubations of brine pool water collected via Niskin bottles.

50 nmol L^{-1} per day (hereafter nM d^{-1}) at 20 and 100 cm, respectively, and were comparable to the rates of AOM on a per-mole basis. As mentioned above, these oxidation rates were measured using water taken from CTD rosette bottles, which, when sampling gas-charged waters, are subject to outgassing and gas phase exchange during recovery. Thus, these rates are considered to be conservative estimates of anaerobic methane oxidation. *In situ* methane oxidation rates are expected to be higher as methane concentrations increase (i.e. on a first-order basis up to k_{max}) and are calculated below.

4.3. Water-column and brine pool methane concentrations

Methane concentrations measured in the water column (Fig. 4) directly above the brine pool ranged from 30 to 70 nM at depths between 2000 and 300 m, representing concentrations that were 15 to 32 times that of atmospheric equilibrium and underscoring the transport of methane from below. At depths below 2000 m, closer to the brine pool, concentrations increased sharply and ranged from 111 to 24 μM. Methane concentrations, as measured by the ISMS approximately 5 cm above the brine fluid/seawater interface near the shore of the pool and 1 cm above the brine fluid/seawater interface in the center of the brine pool, were 180 and 590 μM, respectively. Approximately 1 m above the brine surface, the ISMS-measured methane concentration was ~35 μM, which is in general agreement with the methane concentrations measured in the CTD rosette at this depth (24 μM, well below the saturation of methane at one atmosphere; so these particular Niskin measurements are not compromised by off-gassing (see Fig. 4)). Concentrations at depths of 5, 20, and 80 cm into the brine fluid near the center of the pool were orders of magnitude higher (Fig. 4) with values of 14.3, 20.3, and 33.3 mM, respectively ($\pm 2\%$), and more than an order of magnitude in excess of concentrations measured with Niskin sampling (see Table 1).

5. Discussion

5.1. In situ rates of brine pool anaerobic methane oxidation

The *in situ* rates of AOM reported here exceed values in other anoxic waters by at least one to two orders of magnitude. Our measured rates of AOM from two sampling depths allowed calculation of first-order rate constants of 0.063 and 0.017 yr^{-1} from depths of 20 and 80 cm, respectively. Coupling the *in situ* methane concentration measurements from the ISMS to the aforementioned rate constants yields estimates of the actual rates of AOM of 1285 ± 125 and 572 ± 121 μM yr^{-1} at depths of 20 and 80 cm in the brine pool, respectively. To the best of our knowledge, these AOM rates are by far the highest documented in an anoxic water body. Whereas there has been some evidence that AOM is inhibited by high chloride concentrations (e.g., Joye et al., 2009; Oren, 2002), our data (Tables 1 and 2) suggest that moderately high salinities may in fact not be inhibitory to AOM and that coupled sulfate reduction and AOM may yet play an important role in many Gulf of Mexico hydrocarbon/brine environments.

Many studies have measured AOM in deep-sea environments with high concentrations of methane, and the highest rates are generally found within sediments, particularly hydrate-influenced sediments (e.g., Devol, 1983; Girguis et al., 2003; Joye et al., 2004; Reeburgh, 1980). Indeed, far fewer studies have measured AOM occurring in anoxic water columns, and the rates reported in these studies are generally much lower than sediment rates (as is the case with most biogeochemical processes, primarily because of microbial density being substantially higher in sediments). Rates of AOM measured in the anoxic waters of Cariaco Basin (~1.5 μM yr^{-1}; Ward et al., 1987), Saanich Inlet (7.3 μM yr^{-1}; Ward et al., 1989), and Black Sea (0.6 μM yr^{-1}; Reeburgh et al., 1991) were all orders of magnitude lower than those observed in this study. Joye et al. (1999) measured rates as high as 17.5 μM yr^{-1} in the bottom waters of alkaline, saline Mono Lake. Notably, these rates were measured during a period when the lake waters were well mixed. More recent data collected during a period of extended meromixis in Mono Lake exhibit substantially higher rates of AOM (up to 365 μM yr^{-1}) (Joye et al., 2009).

The rates of AOM presented here are also consistent with the extremely high *in situ* concentrations occurring at these depths. Turnover times of methane in the anaerobic brines were on the order of 16–58 years, more than long enough to maintain supply of SO_4^{-2} via diffusion. Such long turnover times also might suggest that supply to the overlying water via diffusion is likely to be a substantial methane sink relative to removal by AOM (or aerobic oxidation at the brine-seawater interface) in similar brine pool environments. Indeed, given that the rate constants were lower

than in many other comparable environments, the rates presented represent a conservative estimate and, as previously mentioned, the rate constants would likely increase at the higher methane concentrations found *in situ*.

5.2. Estimates of CH_4 flux from the brine pool

Research on deep-sea fluxes and transformations of biological compounds is constantly challenged by the need to sample at extreme temperatures, depths, and pressures. Measurement of these compounds *in situ* provides more rigorous constraints on their fluxes and transformation rates. In the context of the current study, the *in situ* mass spectrometer allowed direct measurement of methane concentrations in a gas-charged brine pool. These concentration measurements were used to calculate a diffusive flux of methane from the brine pool into the overlying water column of 1.1 ± 0.2 mol m^{-2} yr^{-1}, illustrating the magnitude of methane flux from benthic environs into the overlying mixed layer (discussed in detail below).

Specifically, discrete *in situ* measurements taken over a depth profile across the seawater-brine interface provide a context for calculating diffusive geochemical fluxes of methane into the overlying water column. This approach has been used in numerous studies for estimating the mass transfer (e.g., fluxes) of solutes from one region into another. Brine pools such as AC601 are generally very quiescent in nature, with fluid advection playing a small role in controlling fluxes (Joye et al., 2005, 2009). In these locations, where diffusion is the dominant mode of mass transfer, Fick's first law is used to make first-order estimates of the diffusive flux on the basis of measured concentration gradients. The range of possible flux values is based on error in the spatial resolution of the gradient (i.e. since high-precision positioning of the sampling wand was not possible, we estimated the potential vertical position $\times$ 10 cm). Moreover, we adopted a value of $1.38e^{-5}$ cm^2 s^{-1} for the diffusion coefficient of methane in seawater adjusted for the average viscosity of the brine using the Stokes-Einstein relationship (Mao and Duan, 2008; Sahores and Witherspoon, 1970).

Even with our lower bound estimate of diffusive methane flux (1.1 mol m^{-2} yr^{-1}), water-column-integrated methane oxidation rates (Fig. 4) measured directly above the brine pool ($\sim$320 μmol m^{-2} yr^{-1}) indicate that only a very small fraction of methane escaping the brine pool is biologically consumed in the overlying water column (0.02–0.03%). Although it is likely that lateral advection plays a large role in the disconnect between brine pool flux and water column methane oxidation rates above the brine, upper water column concentrations are nonetheless >10 times that of methane in equilibrium with the atmosphere, confirming the transport of methane from depths >2000 m into the mixed layer, where it easily escapes, un-oxidized, into the atmosphere.

Our estimates of diffusive methane flux should be taken as a lower bound on flux from environments such as Gulf of Mexico brine pools. They also underscore the value of *in situ* measurement for constraining methane fluxes. For example, other studies (Lapham et al., 2008; Schmidt et al., 2003) have modeled diffusive and/or advective fluxes from brine seep environments by comparing profiles of a non-conservative solute (e.g., methane) to conservative solutes (e.g., chloride, temperature). Using a 1-D reaction transport model together with chloride and methane profiles, advective methane fluxes of up to 2 mol m^{-2} yr^{-1} were estimated from brine-influenced sediments characterized by a strong advective flow (Lapham et al., 2008). However, these calculated fluxes were based on methane concentrations from sediment cores that had degassed upon collection, and were thus substantially lower than methane concentrations *in situ*. In another study, Solomon et al. (2008) employed osmotic samplers, demonstrating that net seafloor methane fluxes ranged from 0.89 mol m^{-2} yr^{-1} in a mussel bed environment up to 29 mol m^{-2} yr^{-1} in a bacterial mat environment. Heretofore, because methane concentrations could not be reliably determined at *in situ* pressure and temperature, fluxes were calculated assuming that porewater was in equilibrium with methane hydrate under *in situ* conditions. However, others have shown that methane in sediments around hydrate can be far from saturated (Lapham et al., pers. comm.), which would result in much lower flux estimates. Future studies should aim to couple *in situ* methane measurements with direct fluid flow measurements to better constrain the contribution of adjective flux to water column methane flux.

6. Summary and conclusions

Our calculated *in situ* AOM rates, using empirically derived rate constants, are higher than those previously published by one to two orders of magnitude. The diffusive flux was estimated to range as high 1.8 mol m^{-2} yr^{-1} from the brine pool, while integrated oxidation rates in the overlying 2000 m water column could account for only 0.32 μmol m^{-2} yr^{-1}. These data suggest that a very large component of the diffusive brine pool methane flux escapes both aerobic and anaerobic oxidation in the water column above the brine pool and may be released into the atmosphere (or at least subject to dispersion via lateral advection). These first *in situ* measurements of methane concentration from a brine pool using the ISMS enabled robust quantification of methane concentrations at *in situ* conditions in these gas-charged brines and reflect the strong influence of surrounding hydrocarbon seep environments. Such integrated approaches, wherein geochemical determinations are coupled with microbiological activity measurements, are the best means of providing a rigorous constraint on methane diffusive fluxes and transformation rates and will improve our understanding of the role that hydrocarbon seeps may play in the delivery of methane into the ocean and ultimately the atmosphere.

Acknowledgments

We are especially grateful to Stephane Hourdez for his immense help with the Membrane Inlet Mass Spectrometry instrument during this expedition. We are also grateful to Dr. Charles Fisher for his support, as well as to the captains and crew of the *RV Ronald H. Brown* and *RV Atlantis*. Special thanks to the pilots and support staff of the *DSV ALVIN* and *DSV JASON II* from Woods Hole Oceanographic Institution for help in collecting and processing samples. Extra thanks go especially to Matthew Heinz and Tito Collasius for their assistance in the machine shop. This research was supported by the U.S. Department of the Interior BOEMRE, the National Oceanic and Atmospheric Administration, the David and Lucile Packard Foundation, Harvard University, and the National Science Foundation (MCB-0702504).

References

Bell, R.J., Short, R.T., van Amerom, F.H., Byrne, R.H., 2007. Calibration of an in situ Membrane Inlet Mass Spectrometer for measurements of dissolved gases and volatile organics in seawater. Environmental Science & Technology 41 (23), 8123–8128.

Camilli, R., Hemond, H.F., 2004. NEREUS/Kemonaut, a mobile autonomous underwater mass spectrometer. Trends in Analytical Chemistry 23 (4), 307–313.

Carini, S., LeCleir, G., Bano, N., Joye, S.B., 2005. Activity, abundance and diversity of aerobic methanotrophs in an alkaline, hypersaline lake (Mono Lake, CA, USA). Environmental Microbiology 7 (8), 1127–1138.
Childress, J.J., Arp, A.J., Fisher Jr., C.R., 1984. Metabolic and blood characteristics of the hydrothermal vent tubeworm Riftia pachyptila. Marine Biology 83, 109–124.
Collett, T., Kuuskraa, V., 1998. Hydrates contain vast store of world gas resources. Oil Gas Journal 96 (19), 90–95.
Devol, A.H., 1983. Methane oxidation rates in the anaerobic sediments of Saanich Inlet. Limnology and Oceanography 28, 738–742.
Dickens, G.R., 2003. Rethinking the global carbon cycle with a large, dynamic and microbially mediated gas hydrate capacitor. Earth and Planetary Science Letters 213 (3-4), 169–183.
Duan, Z., Mao, S., 2006. A thermodynamic model for calculating methane solubility, density and gas phase composition of methane-bearing aqueous fluids from 273 to 523 K and from 1 to 2000 bar. Geochimica et Cosmochimica Acta 70 (13), 3369–3386.
Fisher, C.R., Roberts, H., Cordes, E.E., Bernard, B., 2007. Cold seeps and associated communities of the Gulf of Mexico. Oceanography 20 (4), 118–129.
Girguis, P.R., Childress, J.J., Freytag, J.A., Klose, K., Stuber, R., 2002. Effects of metabolite uptake on proton-equivalent elimination by two species of deep-sea vestimentiferan tubeworms, *Riftia pachyptila* and *Lamellibrachia luymesi*. Journal of Experimental Biology 205, 3005–3006.
Girguis, P.R., Lee, R.W., Childress, J.J., Pospesel, M., Desaulniers, N.T., Zal, F., Felbeck, H., 2000. Fate of nitrate acquired by the hydrothermal vent tubeworm *Riftia pachyptila*. Applied and Environmental Microbiology 66 (7), 2783–2790.
Girguis, P.R., Orphan, V.J., Hallam, S.J., DeLong, E.F., 2003. Growth and methane oxidation rates of anaerobic methanotrophic archaea in a continuous flow reactor bioreactor. Applied and Environmental Microbiology 69, 5492–5502.
Hemond, H.F., 1991. A backpack-portable mass spectrometer for measurement of volatile compounds in the environment. Review of Scientific Instruments 62 (6), 1420–1425.
Johnson, R., Cooks, R., Allen, T., Cisper, M., Hemberger, P., 2000. Membrane introduction mass spectrometry: Trends and applications. Mass Spectrometry Reviews 19, 1–37.
Joye, S.B., Boetius, A., Orcutt, B.N., Montoya, J.P., Schulz, H.N., Erickson, M.J., Lugo, S., 2004. The anaerobic oxidation of methane and sulfate reduction in sediments from Gulf of Mexico cold seeps. Chemical Geology 205, 219–238.
Joye, S.B., Connell, T.L., Miller, L.G., Oremland, R.S., Jellison, R.S., 1999. Oxidation of ammonia and methane in an alkaline, saline lake. Limnology and Oceanography 44 (1), 178–188.
Joye, S.B., MacDonald, I.R., Montoya, J.P., Peccini, M., 2005. Geophysical and geochemical signatures of Gulf of Mexico seafloor brines. Biogeosciences 2, 295–309.
Joye, S.B., Samarkin, V., Orcutt, B.N., MacDonald, I.R., Hinrichs, K.-U., Elvert, M., Teske, A., Lloyd, K.G., Lever, M.A., Montoya, J.P., Meile, C., 2009. Metabolic variability in seafloor brines revealed by carbon and sulfur cycling. Nature Geosciences 2, 349–354.
Joye, S.B., Bowles, M.W., Samarkin, V.A., Hunter, K.S., Niemann, H., 2010. Biogeochemical signatures and microbial activity of different cold-seep habitats along the Gulf of Mexico deep slope. Deep-Sea Research II 57 (21–23), 1990–2001.
Joye, Samantha B., Samarkin, Vladimir, Bowles, Marshall W., Carini, S.A., Crespo-Medina, M., Madigan, M.T., 2009. Patterns and controls on anaerobic oxidation of methane in extreme environments of varying salinity. Geochimica Cosmochimica Acta Supplement 73, A608.
Kaiser, J., Reuer, M.K., Barnett, B., Bender, M.L., 2005. Marine productivity estimates from continuous O2/Ar ratio measurements by membrane inlet mass spectrometry. Geophysical Research Letters, 32. doi:10.1029/2005GL23459.
Kana, T.M., Darkangelo, C., Hunt, M.D., Oldham, J.B., Bennett, G.E., Cornwell, J., 1994. Membrane Inlet Mass Spectrometer for rapid high-precision determination of N2, O2, Ar in environmental water samples. Analytical Chemistry 66, 4166–4170.
Kana, T.M., Sullivan, M.B., Cornwell, J.C., Groszkowski, K.M., 1998. Denitrification in estuarine sediments determined by membrane inlet mass spectrometry. Limnology and Oceanography 43 (2), 334–339.
Kennicutt II, M.C., Brooks, J.M., Denous, G., 1988. Leakage of deep, reservoired petroleum to the near surface on the Gulf of Mexico continental slope. Marine Chemistry 24, 29–59.
Ketola, R.A., Kotiaho, T., Cisper, M.E., Allen, T.M., 2002. Environmental applications of membrane introduction mass spectrometry. Journal of Mass Spectrometry 37, 457–476.
Kvenvolden, K., 1993. Gas hydrates - geological perspective and global change. Reviews of Geophysics 31 (2), 173–187.
Kvenvolden, K., Lorensen, T.D., 2008. A global inventory of natural gas hydrate occurence. 〈http://walrus.wr.usgs.gov/globalhydrate/index.html〉.
Lapham, L.L., Alperin, M., Chanton, J., Martens, C.S., 2008. Upward advection rates and methane fluxes, oxidation, and sources at two Gulf of Mexico brine seeps. Marine Chemistry 112, 65–71.
Lloyd, D., Davies, K.J., Boddy, L., 1986. Mass spectrometry as an ecological tool for in situ measurement of dissolved gases in sediment systems. FEMS Microbiology Ecology 38, 11–17.
Lloyd, D., Thomas, K.L., Hayes, A., Hill, B., Hales, B.A., Edwards, C., Saunders, J.R., Ritchie, D.A., Upton, M., 1998. Micro-ecology of peat: Minimally invasive analysis using confocal laser scanning microscopy, membrane inlet mass spectrometry and PCR amplification of methanogen-specific gene sequences. FEMS Microbiology Ecology 25, 179–188.
MacDonald, I.R., Reilly, J., Guinasso, J., Brooks, J.M., Carney, R., Bryant, W.A., Bright, T.J., 1990. Chemosynthetic mussels at a brine-filled pockmark in the northern Gulf of Mexico. Science 248 (4959), 1096–1099.
MacDonald, I.R., Sager, W., Peccini, M., 2003. Association of gas hydrate and chemosynthetic fauna in mounded bathymetry at mid-slope hydrocarbon seeps: northern Gulf of Mexico. Marine Geology 198, 133–158.
Mao, Shide, Duan, Zhenhao, 2008. The P, V, T, x properties of binary aqueous solutions up to $T=573$ K and 100 MPa. Journal of Chemical Thermodynamics 40 (7), 1046–1063.
Orcutt, B.N., Boetius, A., Elvert, M., Samarkin, V., Joye, S.B., 2005. Molecular biogeochemistry of sulfate reduction, methanogenesis and the anaerobic oxidation of methane at Gulf of Mexico cold seeps. Geochimica et Cosmochimica Acta 69 (17), 4267–4281.
Oren, A., 2002. Diversity of halophilic microorganisms: environments, phylogeny, physiology, and applications. Journal of Industrial Microbiology and Biotechnology 28, 56–63.
Reeburgh, W.S., 1980. Anaerobic methane oxidation: Rate depth distribution in Skan Bay sediments. Earth and Planetary Science Letters 47 (3), 345–352.
Reeburgh, W.S., 2007. Oceanic methane biogeochemistry. Chemical Reviews 107 (2), 486–513.
Reeburgh, W.S., Ward, Bess B., Whalen, S.C., Sandbeck, K.A., Kilpatrick, K.A., Kerkhof, L.J., 1991. Black Sea methane geochemistry. Deep-Sea Research I. Oceanographic Research Papers 38 (2) SUP (2 p. 1/2), S1189–S1210.
Roberts, H., Carney, R., 1997. Evidence of episodic fluid, gas, and sediment venting on the northern Gulf of Mexico continental slope. Economic Geology 92, 863–879.
Roberts, H., Fisher, C.R., Bernard, B., Brooks, J.M., Bright, M., Carney, R., Cordes, E., Hourdez, S., Hunt, J.J., Joye, S.B., 2007. ALVIN explores the deep northern Gulf of Mexico Slope. EOS Transactions 88, 341–342.
Roberts, H.H., Boland, G.S., 2010. Preface. Deep-Sea Research II 57 (21–23), 1835–1836.
Sahores, J., Witherspoon, P., 1970. Diffusion of light paraffin hydrocarbons in water from 2 to 80 deg C. In: Hobbson, G., Spears, G. (Eds.), Advances in Organic Geochemistry. Permagon Oxford, pp. 219–230.
Schmidt, M., Botz, R., Faber, E., Schmitt, M., Poggenburg, J., Garbe-Schonberg, D., Stoffers, P., 2003. High Resolution methane profiles across anoxic brine-seawater boundaries in the Atlantis II, Discovery, and Kebrit Deeps (Red Sea). Chemical Geology 200, 359–375.
Sloan, L.C., Walker, J.C., Moore, J., TC., Rea, D.K., Zachos, J.C., 1992. Possible methane-induced polar warming in the early Eocene. Nature 357, 320–322.
Solomon, E.A., Kastner, M., Jannasch, H., Robertson, G., Weinstein, Y., 2008. Dynamic fluid flow and chemical fluxes associated with a seafloor gas hydrate deposit on the northern Gulf of Mexico Slope. Earth and Planetary Science Letters 270, 95–105.
Suess, E., Torres, M., Bohrmann, G., Collier, R., Greinert, J., Linke, P., Rehder, G., Trehu, A., Wallman, K., Zuleger, E., 1999. Gas hydrate destablization: Enhanced dewatering, benthic material turnover and large methane plumes at the Cascadia convergent margin. Earth and Planetary Science Letters 170, 1–15.
Tortell, P., 2005a. Small-scale heterogeneity of dissolved gas concentrations in marine continental shelf waters. Geochemistry, Geophysics, Geosystems 6, Q11M04.
Tortell, P.D., 2005b. Dissolved gas measurements in oceanic waters made by membrane inlet mass spectrometry. Limnology and Oceanography: Methods 3, 24–37.
Valentine, D.L., Blanton, D., Reeburgh, W.S., Kastner, M., 2001. Water column methane oxidation adjacent to an area of active hydrate dissociation, Eel River Basin. Geochimca et Cosmochimica Acta 65, 2633–2640.
Ward, B.B., Kilpatrick, K.A., Novelli, P., Scranton, M., 1987. Methane oxidation and methane fluxes in the ocean surface layer and deep anoxic waters. Nature 327, 226–229.
Ward, B.B., Kilpatrick, K.A., Wopat, A., Minnich, E., Lidstrom, M., 1989. Methane oxidation in Saanich Inlet during summer stratification. Continental Shelf Research 9, 65–75.
Zachos, James C., Pagani, Mark, Sloan, Lisa, Thomas, Ellen, Billups, Katharina, 2001. Trends, Rhythms, and Abberations in Global Climate 65 Ma to Present. Science 292 (5517), 686–693.